FEBS Letters

Minireview

Structure–activity relationship of amyloid fibrils

Samir K. Maji [a],*, Lei Wang [b], Jason Greenwald [b], Roland Riek [b],*

[a] School of Bioscience and Bioengineering, IIT-Bombay, Powai, Mumbai 400076, India
[b] ETH Zurich, Physical Chemistry, ETH Honggerberg, 8093 Zurich, Switzerland

ARTICLE INFO

ABSTRACT

Protein aggregation is a process in which proteins self-associate into imperfectly ordered macroscopic entities. Such aggregates are generally classified as either amorphous or highly ordered, the most common form of the latter being amyloid fibrils. Amyloid fibrils composed of cross-β-sheet structure are the pathological hallmarks of several diseases including Alzheimer's disease, but are also associated with functional states such as the fungal HET-s prion. This review aims to summarize the recent high-resolution structural studies of amyloid fibrils in light of their (potential) activities. We propose that the repetitive nature of the cross-β-sheet structure of amyloids is key for their multiple properties: the repeating motifs can translate a rather non-specific interaction into a specific one through cooperativity.

1. Introduction

Rudolf Virchow introduced the term "amyloid" to describe the macroscopic tissue abnormality that exhibits a pale, waxy appearance and produces a positive iodine staining reaction that is characteristic of starch-like materials [1]. The classic histological definition of an amyloid is an extra-cellular protein deposit that binds congo red and produces a yellow-green birefringence under polarized light [2]. Since X-ray fiber diffraction of aligned amyloid fibrils yields a characteristic diffraction pattern with a meridional reflection at 4.7 Å and an equatorial reflection at around 8–11 Å, the underlying organization is proposed to be the cross-β-sheet structural motif [3–5] (Fig. 1). In the cross-β structure, the individual strands of each β-sheet run perpendicular to the fibril axis (4.7 Å spacing) whereas the β-sheets (∼10 Å spacing) are parallel to the fibril axis (Fig. 1). Under the electron microscope (EM), amyloid fibrils appear to be long, non-branched filaments with 6–12 nm diameters, indicating that amyloid fibrils are composed of an ordered arrangement of thousands of copies of a peptide/protein [4] (Fig. 1). These structural characteristics of amyloid fibrils

are used here to redefine the amyloid entity as simply a (fibrillar) protein aggregate with an underlying cross-β-sheet motif. It is the aim of this review to summarize the recently established high-resolution structural data on amyloids and to set this information in perspective with their (biological) activities.

2. Low-resolution structural studies of amyloid fibrils: the cross-β-sheet motif

Since amyloid fibrils are non-crystalline and insoluble in water, detailed structural studies by single crystal X-ray crystallography and multidimensional NMR are difficult (but see below). Hence, low-resolution methods were established for the physical and structural characterization of amyloid fibrils. The initial insight into the secondary structure present in amyloid fibrils came from the tinctorial properties of amyloids in vivo. Congo red binds the amyloid entity and exhibits yellow-green birefringence under cross-polarized light, indicating the presence of ordered structure in the amyloid aggregate [2]. Similarly, amyloid binding-induced Thioflavin T fluorescence suggests the presence of ordered structure in the aggregates [6]. The repetitive nature of the cross-β-sheet structure of amyloids can be assayed by X-ray fiber diffraction [4,5]. Circular dichroism (CD) and Fourier transform infrared spectroscopy (FTIR) are used to measure the β-sheet content of amyloids [7], whereas electron microcopy (EM) can define the boundaries and shape of the amyloid fibrils to a resolution of
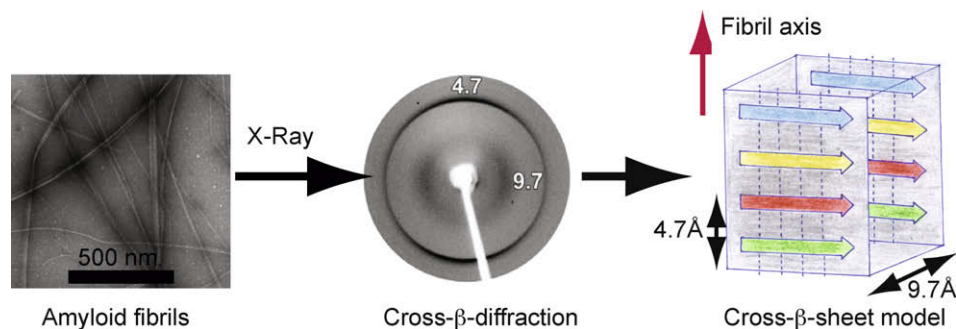
Fig. 1. Amyloid fibrils are composed of long filaments as shown by the transmission electron micrograph. In the fiber diffraction pattern they show a meridional reflection at 4.7 Å and an equatorial reflection at around 8–11 Å, which suggest the presence of a cross-β-sheet structural motif as depicted in the drawing.

approximately 10–25 Å [8–10]. In contrast, electron paramagnetic resonance spectroscopy (EPR) [11] and quenched hydrogen/deuterium exchange coupled with mass spectrometry [12] or two-dimensional nuclear magnetic resonance spectroscopy (NMR) provide significant details about the local structure of the amyloid fibrils [13–15]. By combining the information derived from these methods several structural models have been proposed (for a complete list see Table 1), but these techniques cannot yield atomic resolution structures.

Recent advances in solid-state NMR techniques allow for the accurate measurement of intermolecular distances and backbone torsion angles of amyloid fibrils. Lansbury et al. first described the application of solid-state NMR in determining the anti-parallel nature of Aβ(34–42) fibrils based on intramolecular ^{13}C–^{13}C distances and ^{13}C chemical shifts [16]. Balbach et al. reported multiple-quantum NMR and rotational echo double-resonance results for Aβ(16–22) fibrils that suggested an anti-parallel β-sheet structure [17]. For Aβ(1–40) an in-register parallel β-sheet conformation has been suggested based on multiple-quantum NMR experiments and likewise for Aβ(10–35) by dipolar recoupling in a windowless sequence measurement [18,19]. Tycko and coworkers collected more restraints and established structural models for the polymorphic Aβ(1–40) [20]. Table 1 lists the solid-state NMR studies to date on amyloid fibrils including amyloid fibrils of islet amyloid polypeptide (IAPP), α-synuclein, prion protein, and a WW domain.

3. X-ray crystallography: the 3D structure of the cross-β-spine of short amyloidogenic peptides

Recently, Eisenberg et al. determined the 3D structures of short fibril-forming peptide segments of amyloid proteins (i.e. Sup35, insulin, Aβ, tau, and amylin) by X-ray crystallography [21,22]. The peptides that they studied are highly soluble in water, but are also able to form microcrystals as well as fibrils. Using a specially designed microfocus beamline, the researchers were able to elucidate several high-resolution structures from these microcrystals. Interestingly, they are composed of the cross-β-sheet motif that is proposed to be the core structure of amyloid fibrils. Several experimental results support the notion that the peptide conformation in the microcrystals could be shared with the fibril structure: microcrystals and fibrils grow in the same condition and coexist in the same solution; some fibrils grow from the tips of crystals; and the microcrystals can seed the growth of amyloid fibrils. Moreover, the powder diffraction patterns of microcrystals and their fibril counterparts are very similar.

In the initial X-ray structure determined from microcrystals of the peptide GNNQQNY from Sup35, the peptides form perfectly in-register β-sheets parallel to the short (4.86 Å) edge of the unit cell (but the long axis of the microcrystal) (Fig 2). Similar to their

expected orientation in a fibril, the individual β-strands are perpendicular to the long axis of the microcrystal. The β-sheets are packed in the crystal with two distinct interfaces, termed the "dry" and "wet" interfaces (Fig. 3). The dry interface consists of side chain interdigitation of complementary side chains via van der Waal's interactions and hydrogen bonds typical of Asn/Gln ladders [20–22]. This structural motif is called the "steric zipper" and has also been documented for Aβ(1–42) fibrils [9,20]. In contrast to the dry interface, the wet interface is composed mainly of hydrogen bonds between the sidechains and also via water molecules in a fashion that is similar to intermolecular contacts in protein crystals. This suggests that the stable structural unit of the microcrystals is a pair of β-sheets forming a minimal cross-β-sheet motif.

Eisenberg et al. have since reported on another dozen high-resolution microcrystal structures from peptides with a variety of amino-acid sequences, and more will come (Table 2). All of the structures are in an "infinite" β-sheet conformation with the sheets forming an interface via a steric zipper [22] demonstrating the prevalence of the cross-β-sheet motif with steric zipper-type side chain interactions in peptide complementation and oligomerization in amyloid fibrils. However, there are important differences between the various structures and according to these differences, the steric zippers can be categorized by (i) whether their β-strands are parallel or anti-parallel, (ii) whether their β-sheets pack with the same ('fact to face") or different ('face-to-back') surfaces adjacent to one another, and (iii) whether the two closely packed β-sheets are oriented in the same direction ('up–up') or opposite direction ('up–down'). Combinations of these three structural arrangements give eight theoretically possible classes of steric zippers of which five were observed experimentally. Interestingly, some peptides can form different microcrystals comprising different classes of steric zippers, offering a molecular-level explanation for amyloid polymorphism [23–25] and prion strains [15,26].

Although the crystal structures may indicate that the structural complexity of amyloid fibrils is limited, it is noteworthy to mention that only peptides and not entire proteins were crystallized so far in an amyloid-like conformation, and hence, one should not underestimate the possible structural complexity of protein fibrils (but see [11]). In particular, a complex structure might be derived from a combination of steric zipper-like structures composed by several peptide segments within a single polypeptide chain as exemplified by the 3D structure of the HET-s(218–289) amyloid fibrils discussed next.

4. Solid-state NMR: the 3D structure of HET-s(218–289) amyloid fibrils

The 3D structure of HET-s(218–289) amyloid fibrils has been determined by solid-state NMR [27]. High-resolution solid-state

Table 1
Structural studies of amyloids by solid state and solution state NMR spectroscopy.

Protein/peptide	No. of amino acids	NMR	Structural information	References
Aβ(34–42)	9	Solid state	Antiparallel β-sheet	[16]
Aβ(10–35)	26	Solid state	Parallel β-sheet	[18,19,70]
Aβ(16–22)	7	Solid state	Antiparallel β-sheet	[17]
TTR(105–115)	11	Solid state	Extended β-sheet, 3D structure of a single peptide chain	[71]
Aβ(1–42)	42	Solid state	Parallel β-sheet	[70]
Aβ(11-25)	15	Solid state	Antiparallel β-sheet	[72]
[M35ox]Aβ42	42	H/D exchange	Parallel β-sheet, cross-β-sheet with steric zipper	[9]
Peptide ccβ	17	Solid state	Anti parallel β-sheet	[73]
β₂M	97	H/D exchange	β-sheet core of the fibrils	[13]
β₂M(20–41)	22	Solid state	Parallel β-sheet, cross-β-sheet with steric zipper	[74]
HET-s(218–289)	72	H/D exchange and solid state	β-solenoid structure (see text)	[27]
Aβ40	40	Solid state	Parallel β-sheet, cross-β-sheet with steric zipper	[20]
[D23 N]Aβ40	40	Solid state	Polymorphism of in-registrar parallel (minor) and anti-parallel (major) β-sheet structure	[75]
Brain-seeded synthetic Aβ40	40	Solid state	Parallel β-sheet	[76]
α-Synuclein	140	Solid state	β-Sheet-rich fibril core of residues 38–95	[77]
α-Synuclein	140	H/D exchange and solid state	The fibril core of residues 30–110 with five β-strands	[10]
Ure2p(1–89)	89	Solid state	Parallel β-sheet	[78]
Ure2p(10–39)	30	Solid state	Parallel β-sheet with polar zipper	[79]
IAPP	37	Solid state	Parallel β-sheet comprising β-strand of residue 8–17 and 28–37	[80]
hIAPP(20–29)	10	Solid state	Antiparallel β-sheet	[81]
hIAPP(20–29)	10	Solid state	Polymorphism between parallel and antiparallel β-sheet depending on sample preparation	[82]
Sup35(1–253)	253	Solid state	Parallel β-sheet	[83]
Rnq1(153–405)	253	Solid state	Parallel in-registrar β-sheet	[84]
huPrP(23–144)	122	Solid state	Fibril core comprising residues 112–141 with β-strands	[85]
mPrP(89–143)P101L	55	Solid state	β-Sheet conformation comprising residues 112–124	[86,87]
moPrP(106–126)	21	H/D exchange	β-Sheet conformation comprising residues of 112–124	[88]
WW domain of Human CA150	37	Solid state	Parallel β-sheet, cross-β-sheet	[89]
Sup35 (Sup NM), Sc4 and Sc37 strains	253	H/D Exchange	Overlapping amyloid core of Sup1–40 and strain dependent expansion of protection for Sc37	[15]
TTRY114C	128	H/D Exchange	Fibril core comprised of the six β–strands, which retains a native-like conformation	[90]
Aβ(1–42)	42	H/D Exchange	Fibril core comprising residues 11–25 and 28–42	[91]
Aβ(1–40)	40	H/D Exchange	Fibril core comprising residues 8–25 and 27–40, and partially protected residues 4–5	[92]
ccβ-p	17	Solid state	At low pH: −2 out-of-register antiparallel β-sheet At neutral pH: +3 out-of-register antiparallel β-sheet	[93]
CspA	70	H/D Exchange	The entire CspA polypeptide chain is structured in the fibrils	[94]
Aβ(25–35)	11	H/D Exchange	Fibril core comprising residues 28–35	[95]
AMed42–49	8	Solid state	A parallel in-register arrangement within β-sheets	[96]
HamsterPrP(109–122)	14	Solid state	Steric zipper-like β-sheet	[97]
apoC-II	79	H/D Exchange	Fibril core comprising residues 19–37 and 57–74	[98]
Aβ(14–23)	10	Solid state	Antiparallel β-sheets	[99]
Aβ(1–40)	40	H/D Exchange	Fibril core comprising residues 16–24 and 27–36	[100]
hCT	32	Solid state	Antiparallel β-sheets	[101]

NMR spectra of $^{13}C,^{15}N$-labeled HET-s(218–289) fibrils were recorded for sequence-specific assignment and the collection of distance and angular restraints. The resonance lines are strikingly narrow (down to 0.2 ppm) and are comparable to those of microcrystalline proteins, indicating a highly ordered structure for a part of the fibrils. Upon sequence-specific chemical shift assignment, the secondary structure could be determined by the deviations of the combined ^{13}C chemical shifts from random coil values. Negative deviations indicated β-sheet secondary structure for residues 226–234, 237–244, 262–271 and 273–282. Exceptions were observed at residues 229 and 265 (see below) and, to a lesser degree, at 277. The striking correlation between the quenched H/D exchange data and the chemical shift data allowed for the confident establishment of secondary structure in the HET-s(218–289) amyloid fibrils [14]. Subsequently, the 3D structure of HET-s(218–289) amyloid fibrils was determined using 134 experimental inter- and intramolecular distance restraints collected in PDSD (proton-driven ^{13}C spin diffusion) experiments [27]. The refined model shows that HET-s(218–289) forms a left-handed β-solenoid, with each molecule forming two helical windings. The four β-strands com-

prising residues 226–234 (β1), 237–245 (β2), 262–270 (β3) and 273–282 (β4) are connected by two short loops (β1–β2 and β3–β4) and by an unstructured 15-residue-long segment between β2 and β3 (Fig. 2b). The high level of structural order and the stability of HET-s(218–289) fibrils are explained by the formation of the compact hydrophobic core, at least 23 hydrogen bonds per molecule, three salt-bridges and two asparagine-ladders.

The β-solenoid structure of the HET-s(218–289) fibrils (Fig. 2) is composed of a combination of structural entities observed in the crystal structures of the amyloid peptides (see above). In particular, the four β-sheets of HET-s(218–289) fibrils are parallel and in-register. The interactions between three strands are of hydrophobic nature accompanied at the arches by several hydrogen bonds and an Asn ladder consisting of residues N226/N262. The surface residues are mostly charged and form several salt-bridges. These structural arrangements result in an overall β-helix characteristic fold, which is of much higher structural complexity than short peptide fibrils – a complexity, which is typically observed in soluble protein folds. Indeed, the three-stranded triangular hydrophobic core superimposes well with the β-solenoid
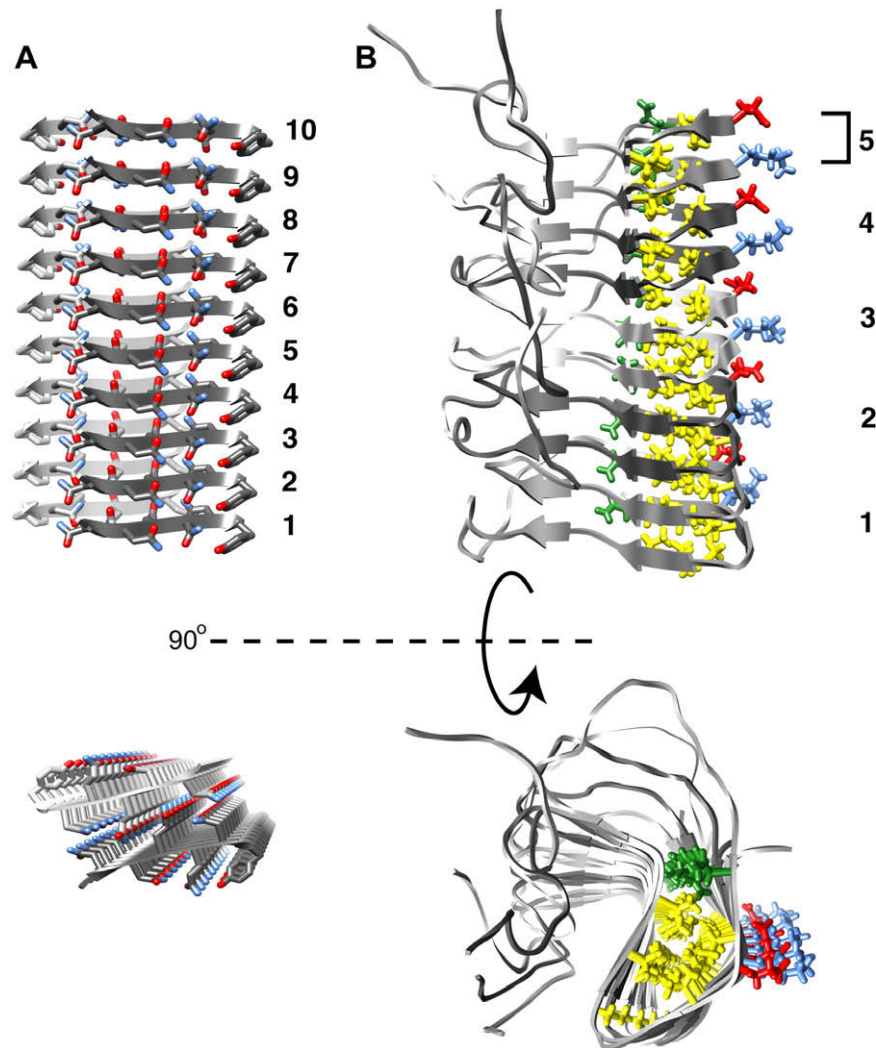
Fig. 2. 3D structures of the (A) x-ray structure of the peptide GNNQQNY and (B) the NMR structure of HET-s(218–289). The β-strands are indicated by grey arrows. In (A) all side chains are shown and the atoms are color coded red for oxygen and blue for nitrogen, respectively. In (B) only a few side chains were selected for simplicity: The side chains of the hydrophobic core are colored yellow. The Asn ladder of residues N226/N262 is in green, and the salt bridge between Lys229 (blue) and Glu265 (red) is also shown.

structures of soluble proteins, such as the tailspike protein P22 [28], and the filamentous hemagglutinin, a 230 kDa adhesion of the whooping cough agent *Bordetella pertussis* [29].

5. Structure–activity relationship of HET-s(218–289) amyloid fibrils

The well-organized structure of the HET-s prion fibrils is evident and supports the proposed native function of the amyloid state to be an infectious entity [14,30]. This interpretation is demonstrated by the presence of the two pseudo-repeats in the sequence. The repeats provide intramolecular hydrogen bonds that may facilitate the nucleation and growth of fibrils [14], while the differences between the two repeat sequences support the fibril fold. In particular, K229 in β1 with E265 in β3, E234 in β1 with K270 in β3, and K236 in β2 with E272 in β4 form charge-compensating salt-bridges (Fig. 2), which in a perfectly repeated sequence would result in charge-repulsion. These charge alterations along the fibril axis also support the correct in-register alignment of the β-sheets resulting in a single packing scheme that may explain the extraordinarily high order in these fibrils, as seen by NMR, as

well as the absence of polymorphism in HET-s fibrils grown at physiological pH [27]. Furthermore, the solvent-exposed side chains are hydrophilic making the HET-s(218–289) fibrils reminiscent of soluble proteins. This property may be beneficial for and accelerate prion propagation, because it will support the diffusion of the prion fibril by suppressing non-specific hydrophobic interactions with other proteins or the membrane. Since these interactions have been suggested to be possible toxic mechanisms of disease-associated amyloids or the prefibrillar aggregates thereof [31], it is intriguing to speculate whether HET-s fibrils are non-toxic because of their charge-compensated hydrophilic surface.

The detailed structural analysis of HET-s(218–289) amyloids established the structure of the infectious form of a prion protein at atomic resolution. Alteration of the structure by the introduction of the β-sheet breaking Pro residue at β-strand locations resulted in a loss of infectivity in the fungus [14] indicating that the structure of the amyloid appears to be the infectious entity of the HET-s prion [14]. Whether this structural entity helps in elucidating the mechanism of prion formation and propagation of the other yeast and mammalian prions remains to be seen [15,32,33]. The evolutionarily optimized fibril structure of HET-s(218–289) serves also
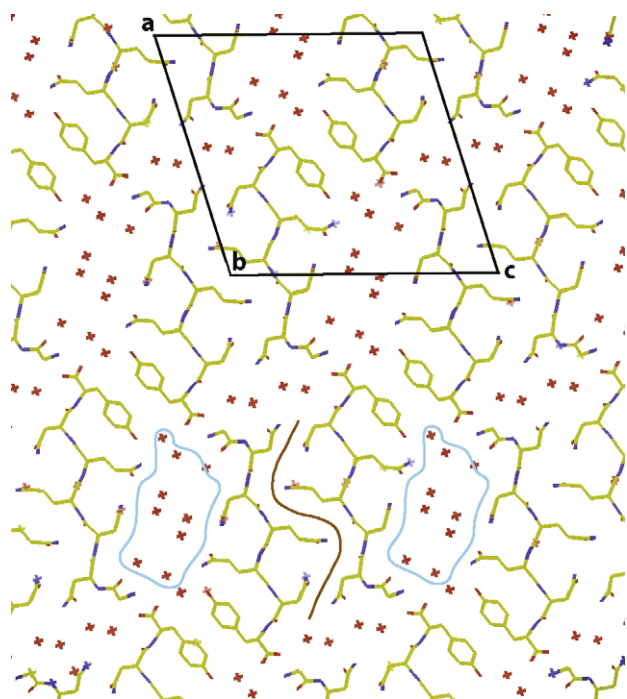
Fig. 3. Crystal packing for the peptide GNNQQNY (PDB entry 1YJP) viewed along the b axis so that the β-sheets are perpendicular to the page. A single dry interface is depicted with the brown line and two identical wet interfaces are depicted with the blue lines. The unit cell is shown in black.

as a prototypical fibril fold for functional amyloids [34–36] and contrasts in many respects with the disease-associated amyloids discussed in the following text.

6. Disease and functional activities of amyloids

Amyloid fibrils are associated with more than two-dozen human diseases including Alzheimer's, Parkinson's and prion diseases [37]. In striking contrast to the disease-associated amyloids, there are also amyloids with native biological activities [35]. *Escherichia coli* form extra-cellular amyloid fibrils called curli that are involved in surface and cell–cell contacts promoting community behavior and host colonization [36]. The eggshell protein (chorin) of silkworm is an amyloid that protects the oocyte and the developing embryo from a wide range of environmental hazards [38]. The prion amyloids in yeast are associated with enhanced survival of the host in certain environmental conditions [39,40]. The HET-s

prion protein of the fungus Podospora anserina forms infectious amyloids that are involved in a native function called heterokaryon incompatibility [30]. The Pmel17 forms a functional human amyloid that appears to be important in the formation of skin pigmentation [34].

Although it is apparent that the activity of functional, non-toxic and disease-associated, toxic amyloids must be attributed to their 3D structure, there is little or no knowledge about the structural differences responsible for the differences in toxicity. As highlighted above, the lack of toxicity of the functional HET-s fibrils might be due to their hydrophilic surface that may suppress non-specific hydrophobic interactions with other proteins or the membrane. Alternatively, functional amyloid proteins may aggregate into highly specific amyloid fibrils without the presence of conformational intermediates such as protofibrils and oligomers that have been suggested to be the toxic species in Alzheimer's disease ([41–43]). Although still largely composed of β-sheet [44], these conformational intermediates display a common structural motif that is distinct from fibrils as evidenced by the establishment of both oligomer-specific and fibril-specific antibodies [45]. Following this hypothesis, it has been suggested that the disease-associated amyloid fibrils have a beneficial function by sequestering the toxic oligomers formed during aggregation into a non-toxic mature amyloid [42].

7. Structure–activity relationship of amyloids

Although all amyloids share the cross-β-sheet structural motif, they comprise a variety of biophysical and biological properties. The formation of amyloids may result both in a loss of function of the polypeptide involved as described for the yeast prions [39,40], or a gain of function as in the case of the HET-s prion system [30]. Pmel17 amyloids serve as a template for ligand binding [34] while other amyloids induce a specific toxic response as shown for the HET-s prion system [30]. Prion amyloids are infectious [14] while other amyloids are not (see [46]), and it is variations in the amyloid structure that are responsible for prion strain diversity [15]. Some amyloids can be very stable in harsh physical and biochemical environments while others release readily monomers [47]. Some polypeptides form amyloids at physiological conditions, others only at extreme (non-physiological) conditions. Amyloids are very specific in their aggregation behavior and normally incorporate only a single polypeptide sequence, although coaggregation is possible in certain circumstances [48,49]. The simple fold of a cross-β-structure, being a one-dimensional crystal that can grow indefinitely, still allows for a plurality of properties. In fact, the repetitive nature may be the key for their multiple activities, because the repetitive confor-

Table 2
3D structures of amyloid peptides forming a cross-β-sheet motif.

Peptide sequence	Segment from protein	Type of β-sheet	Type of cross-β-spine	References
GNNQQNY	Sup35	Parallel	Class 1 and class 2	[21,22]
NNQQNY	Sup35	Parallel	Class 2	[21,22]
NNQQ	Sup35	Parallel	Class 2, class 4	[22]
VQIVYK	Tau	Parallel	Class 2	[22]
SSTSAA	RNase	Parallel	Class 1	[22]
SNQNNF	Prion protein	Parallel	Class 2	[22]
GGVVIA	Aβ	Parallel	Class 4	[22]
MVGGVV	Aβ	Antiparallel	Class 8	[22]
LYQLEN	Insulin	Antiparallel	Class 7	[22]
VEALYL	Insulin	Antiparallel	Class 7	[22]
NNFGAIL	Amylin	Parallel	Non-typical steric zipper	[69]
SSTNVG	Amylin	Parallel	Class 1	[69]

Nomenclature [22]: Class 1: parallel, face-to-face, up–up packing; Class 2: parallel, face-to-back, up–up packing; Class 4: parallel, face-to-back, up–down packing; Class 7: antiparallel, face-to-back, up–up packing; Class 8: antiparallel, face-to-back, up–down packing.

mation is able to translate a rather non-specific function into a specific one by cooperativity.

8. Anfinsen's hypothesis

The existence of amyloids emphasizes that Anfinsen's thermodynamic hypothesis [50] must be view in a more general way than is common. Anfinsen stated his hypothesis as: "[T]he three-dimensional structure of a native protein in its normal physiological milieu (solvent, pH, ionic strength, presence of other components such as metal ions or prosthetic groups, temperature, and other) is the one in which the Gibbs free energy of the whole system is lowest; that is, …the native conformation is determined by the totality of interatomic interactions and hence by the amino-acid sequence, in a given environment". Clearly, the amyloid proteins/peptides and in particular the functional amyloid polypeptides have (at least) two stable conformational states: the soluble-monomeric and the insoluble-fibrillar. Because the free energy of a solution depends on the concentration of the solute, the state of the solute can change with its concentration. Thus, it is completely in accord with Anfinsen's hypothesis that the amyloid proteins/peptides occupy one structure in a dilute solution, and another structure – the amyloid state when they are at high concentration. In other words, for many proteins the amyloid state is the thermodynamically stable state at high concentrations, a situation stabilized by a high density of intermolecular hydrogen bonds and complementary steric interactions. Meanwhile, the amyloid state is not the energetically most favorable conformation at a lower protein/peptide concentration.

9. Amyloid aggregation is not a generic property of the peptide backbone

Many proteins aggregate into amyloid-like inclusion bodies when over-expressed in *E. coli* [51,52], while others can aggregate into amyloid-like structures when heat precipitated. Still others that are normally in a soluble form exclusively can be coaxed into amyloid fibrils in the right conditions [53,54]. Despite the fact that so many proteins can achieve an amyloid or amyloid-like conformation, this is not evidence that the formation of amyloid fibrils is mainly a generic property of the polypeptide backbone and that the side chains play a minor role, as has been suggested by Dobson et al. [55]. On the contrary, amyloid aggregation is highly amino-acid sequence specific as demonstrated by the intermolecular side chain interactions observed in the crystal structures of the Eisenberg group [21,22,56]. Furthermore, the essential involvement of side chain interactions in the aggregation process is evident from the observed sequence-specific nature of amyloid aggregation [57–59], and by the experimentally-derived scale of amino-acid aggregation-propensities (ranging from the aggregation-prone hydrophobic residues to the aggregation-interfering charged side chains [60,61]). However, through an exhaustive screening of non-physiological conditions such as extreme protein concentration, a pH less than 3, or the addition of aprotic solvents [53,54,62,63], the influence of the side chains in the aggregation process can be altered or their importance diminished, eventually driving the protein of interest into amyloid fibrils. Although the amyloid-like conformation is one of the common features of many protein aggregates, proteins can also aggregate by domain-swapping [56,64,65], into nanotube structures [66], and into helical assemblies [67,68], all without forming any cross-β structures.

10. Conclusion

Almost 75 years ago, the pioneering biophysicist Astbury published an X-ray diffraction pattern from poached, stretched egg white which had reflections at 4.7 Å in the meridional direction and ∼10 Å along the equatorial direction [3]. The pattern suggested that the protein chains of the egg white pack in an extended or β-conformation, with the chains perpendicular to the long (stretched) axis. The authors concluded that when proteins/peptides aggregate, they go into their energetically most favorable conformational state, this being the cross-β-sheet motif. Now it appears that the egg white example was not a special case and that when proteins aggregate they often form an amyloid-like entity comprising a specific structure. The process of protein aggregation can thus be viewed as a primitive folding mechanism, resulting in a defined aggregated conformation composed of intermolecular hydrogen bonds and side chain – side chain interactions. This in turn determines for each (amyloid) aggregate its own distinct properties, which can include both functional and toxic activities.

References

[1] Sipe, J.D. and Cohen, A.S. (2000) Review: history of the amyloid fibril. J. Struct. Biol. 130, 88–98.
[2] Westermark, G.T., Johnson, K.H. and Westermark, P. (1999) Staining methods for identification of amyloid in tissue. Meth. Enzymol. 309, 3–25.
[3] Astbury, W.T., Dickinson, S. and Bailey, K. (1935) CCLXXIX. The X-ray interpretation of denaturation and the structure of the seed globulins. Biochem. J. 29, 2351–2360.
[4] Sunde, M. and Blake, C. (1997) The structure of amyloid fibrils by electron microscopy and X-ray diffraction. Adv. Protein. Chem. 50, 123–159.
[5] Sunde, M., Serpell, L.C., Bartlam, M., Fraser, P.E., Pepys, M.B. and Blake, C.C. (1997) Common core structure of amyloid fibrils by synchrotron X-ray diffraction. J. Mol. Biol. 273, 729–739.
[6] LeVine, H. (1999) Quantification of β-sheet amyloid fibril structures with thioflavin T. Meth. Enzymol. 309, 274–284.
[7] Fradinger, E.A., Maji, S.K., Lazo, N.D. and Teplow, D.B. (2005) Studying amyloid beta-protein assembly in: Amyloid Precursor Protein (Xu, W.X.a.H., Ed.), pp. 83–110, CRC Press, Boca Ration, London, New York, Washington, DC.
[8] Zhang, R., Hu, X., Khant, H., Ludtke, S.J., Chiu, W., Schmid, M.F., Frieden, C. and Lee, J.M. (2009) Interprotofilament interactions between Alzheimer's Abeta1–42 peptides in amyloid fibrils revealed by cryoEM. Proc. Natl. Acad. Sci. USA 106, 4653–4658.
[9] Luhrs, T., Ritter, C., Adrian, M., Riek-Loher, D., Bohrmann, B., Dobeli, H., Schubert, D. and Riek, R. (2005) 3D structure of Alzheimer's amyloid-beta(1–42) fibrils. Proc. Natl. Acad. Sci. USA 102, 17342–17347.
[10] Vilar, M., Chou, H.T., Lührs, T., Maji, S.K., Riek-Loher, D., Verel, R., Manning, G., Stahlberg, H. and Riek, R. (2008) The fold of alpha-synuclein fibrils. Proc. Natl. Acad. Sci. USA 105, 8637–8642.
[11] Margittai, M. and Langen, R. (2008) Fibrils with parallel in-register structure constitute a major class of amyloid fibrils: molecular insights from electron paramagnetic resonance spectroscopy. Q. Rev. Biophys. 41, 265–297.
[12] Kheterpal, I., Cook, K.D. and Wetzel, R. (2006) Hydrogen/deuterium exchange mass spectrometry analysis of protein aggregates. Meth. Enzymol. 413, 140–166.
[13] Hoshino, M., Katou, H., Hagihara, Y., Hasegawa, K., Naiki, H. and Goto, Y. (2002) Mapping the core of the beta(2)-microglobulin amyloid fibril by H/D exchange. Nat. Struct. Biol. 9, 332–336.
[14] Ritter, C., Maddelein, M.L., Siemer, A.B., Luhrs, T., Ernst, M., Meier, B.H., Saupe, S.J. and Riek, R. (2005) Correlation of structural elements and infectivity of the HET-s prion. Nature 435, 844–848.
[15] Toyama, B.H., Kelly, M.J., Gross, J.D. and Weissman, J.S. (2007) The structural basis of yeast prion strain variants. Nature 449, 233–237.
[16] Lansbury Jr., P.T., Costa, P.R., Griffiths, J.M., Simon, E.J., Auger, M., Halverson, K.J., Kocisko, D.A., Hendsch, Z.S., Ashburn, T.T., Spencer, R.G., et al. (1995) Structural model for the β-amyloid fibril based on interstrand alignment of an antiparallel β-sheet comprising a C-terminal peptide. Nat. Struct. Biol. 2, 990–998.
[17] Balbach, J.J., Ishii, Y., Antzutkin, O.N., Leapman, R.D., Rizzo, N.W., Dyda, F., Reed, J. and Tycko, R. (2000) Amyloid fibril formation by Ab(16–22), a seven-residue fragment of the Alzheimer's b-amyloid peptide, and structural characterization by solid state NMR. Biochemistry 39, 13748–13759.
[18] Benzinger, T.L.S., Gregory, D.M., Burkoth, T.S., Millerauer, H., Lynn, D.G., Botto, R.E. and Meredith, S.C. (1998) Propagating structure of Alzheimers β-amyloid((10–35)) is parallel β-sheet with residues in exact register. Proc. Natl. Acad. Sci. USA 95, 13407–13412.

[19] Benzinger, T.L.S., Gregory, D.M., Burkoth, T.S., Miller-Auer, H., Lynn, D.G., Botto, R.E. and Meredith, S.C. (2000) Two-dimensional structure of b-amyloid (10–35) fibrils. Biochemistry 39, 3491–3499.

[20] Petkova, A.T., Ishii, Y., Balbach, J.J., Antzutkin, O.N., Leapman, R.D., Delaglio, F. and Tycko, R. (2002) A structural model for Alzheimer's β-amyloid fibrils based on experimental constraints from solid state NMR. Proc. Natl. Acad. Sci. USA 99, 16742–16747.

[21] Nelson, R., Sawaya, M.R., Balbirnie, M., Madsen, A.O., Riekel, C., Grothe, R. and Eisenberg, D. (2005) Structure of the cross-beta spine of amyloid-like fibrils. Nature 435, 773–778.

[22] Sawaya, M.R., Sambashivan, S., Nelson, R., Ivanova, M.I., Sievers, S.A., Apostol, M.I., Thompson, M.J., Balbirnie, M., Wiltzius, J.J., McFarlane, H.T., Madsen, A.O., Riekel, C. and Eisenberg, D. (2007) Atomic structures of amyloid cross-beta spines reveal varied steric zippers. Nature 447, 453–457.

[23] Paravastu, A.K., Leapman, R.D., Yau, W.M. and Tycko, R. (2008) Molecular structural basis for polymorphism in Alzheimer's beta-amyloid fibrils. Proc. Natl. Acad. Sci. USA 105, 18349–18354.

[24] Petkova, A.T., Leapman, R.D., Guo, Z., Yau, W.M., Mattson, M.P. and Tycko, R. (2005) Self-propagating, molecular-level polymorphism in Alzheimer's beta-amyloid fibrils. Science 307, 262–265.

[25] Meinhardt, J., Sachse, C., Hortschansky, P., Grigorieff, N. and Fändrich, M. (2009) Abeta(1–40) fibril polymorphism implies diverse interaction patterns in amyloid fibrils. J. Mol. Biol. 386, 869–877.

[26] Tanaka, M., Chien, P., Yonekura, K. and Weissman, J.S. (2005) Mechanism of cross-species prion transmission: an infectious conformation compatible with two highly divergent yeast prion proteins. Cell 121, 49–62.

[27] Wasmer, C., Lange, A., Van Melckebeke, H., Siemer, A.B., Riek, R. and Meier, B.H. (2008) Amyloid fibrils of the HET-s(218–289) prion form a beta solenoid with a triangular hydrophobic core. Science 319, 1523–1526.

[28] Steinbacher, S., Baxa, U., Miller, S., Weintraub, A., Seckler, R. and Huber, R. (1996) Crystal structure of phage P22 tailspike protein complexed with *Salmonella* sp. O-antigen receptors. Proc. Natl. Acad. Sci. USA 93, 10584–10588.

[29] Clantin, B., Hodak, H., Willery, E., Locht, C., Jacob-Dubuisson, F. and Villeret, V. (2004) The crystal structure of filamentous hemagglutinin secretion domain and its implications for the two-partner secretion pathway. Proc. Natl. Acad. Sci. USA 101, 6194–6199.

[30] Maddelein, M.L., Dos Reis, S., Duvezin-Caubet, S., Coulary-Salin, B. and Saupe, S.J. (2002) Amyloid aggregates of the HET-s prion protein are infectious. Proc. Natl. Acad. Sci. USA 99, 7402–7407.

[31] Sokolov, Y., Kozak, J.A., Kayed, R., Chanturiya, A., Glabe, C. and Hall, J.E. (2006) Soluble amyloid oligomers increase bilayer conductance by altering dielectric structure. J. Gen. Physiol. 128, 637–647.

[32] Prusiner, S.B. (1982) Novel proteinaceous infectious particles cause scrapie. Science 216, 136–144.

[33] Krishnan, R. and Lindquist, S.L. (2005) Structural insights into a yeast prion illuminate nucleation and strain diversity. Nature 435, 765–772.

[34] Fowler, D.M., Koulov, A.V., Alory-Jost, C., Marks, M.S., Balch, W.E. and Kelly, J.W. (2006) Functional amyloid formation within mammalian tissue. PLoS Biol. 4, e6.

[35] Fowler, D.M., Koulov, A.V., Balch, W.E. and Kelly, J.W. (2007) Functional amyloid–from bacteria to humans. Trends Biochem. Sci. 32, 217–224.

[36] Barnhart, M.M. and Chapman, M.R. (2006) Curli biogenesis and function. Annu. Rev. Microbiol. 60, 131–147.

[37] Chiti, F. and Dobson, C.M. (2006) Protein misfolding, functional amyloid, and human disease. Annu. Rev. Biochem. 75, 333–366.

[38] Iconomidou, V.A., Vriend, G. and Hamodrakas, S.J. (2000) Amyloids protect the silkmoth oocyte and embryo. FEBS Lett. 479, 141–145.

[39] Osherovich, L.Z. and Weissman, J.S. (2002) The utility of prions. Dev. Cell 2, 143–151.

[40] Maji, S.K., Perrin, M.H, Sawaya, M.R., Jessberger, S., Vadodaria, K., Rissman, R.A., Singru, P. S., Nilsson, K.P.R., Simon, R., Schubert, D., Eisenberg, D., Rivier, J., Sawchenko, P., Vale, W. and Riek R. (2009) Functional amyloids as natural storage of peptide hormones in pituitary secretory granules. Science (on line).

[41] Klein, W.L., Stine Jr., W.B. and Teplow, D.B. (2004) Small assemblies of unmodified amyloid β-protein are the proximate neurotoxin in Alzheimer's disease. Neurobiol. Aging 25, 569–580.

[42] Hardy, J. and Selkoe, D.J. (2002) The amyloid hypothesis of Alzheimer's disease: progress and problems on the road to therapeutics. Science 297, 353–356.

[43] Lazo, N.D., Maji, S.K., Fradinger, E.A., Bitan, G. and Teplow, D.B. (2005) The amyloid beta protein in: Amyloid Protein – The Beta Sheet Conformation and Disease (Sipe, J.D., Ed.), pp. 385–491, Wiley–VCH Publishers, Weinheim, Germany.

[44] Chimon, S., Shaibat, M.A., Jones, C.R., Calero, D.C., Aizezi, B. and Ishii, Y. (2007) Evidence of fibril-like beta-sheet structures in a neurotoxic amyloid intermediate of Alzheimer's beta-amyloid. Nat. Struct. Mol. Biol. 14, 1157–1164.

[45] Kayed, R., Head, E., Thompson, J.L., McIntire, T.M., Milton, S.C., Cotman, C.W. and Glabe, C.G. (2003) Common structure of soluble amyloid oligomers implies common mechanism of pathogenesis. Science 300, 486–489.

[46] Riek, R. (2006) Cell biology: infectious Alzheimer's disease? Nature 444, 429–431.

[47] Maji, S.K., Schubert, D., Rivier, C., Lee, S., Rivier, J.E. and Riek, R. (2008) Amyloid as a depot for the formulation of long-acting drugs. PloS Biol. 6, e17.

[48] Han, H.Y., Weinreb, P.H. and Lansbury, P.T. (1995) The core Alzheimer's peptide Nac forms amyloid fibrils which seed and are seeded by β-Amyloid – is Nac a common trigger or target in neurodegenerative disease? Chem. Biol. 2, 163–169.

[49] Giasson, B.I., Forman, M.S., Higuchi, M., Golbe, L.I., Graves, C.L., Kotzbauer, P.T., Trojanowski, J.Q. and Lee, V.M.Y. (2003) Initiation and synergistic fibrillization of tau and alpha-synuclein. Science 300, 636–640.

[50] Anfinsen, C.B. (1973) Principles that govern the folding of protein chains. Science 181, 223–230.

[51] Ventura, S. and Villaverde, A. (2006) Protein quality in bacterial inclusion bodies. Trends Biotechnol. 24, 179–185.

[52] Wang, L., Maji, S.K., Sawaya, M.R., Eisenberg, D. and Riek, R. (2008) Bacterial inclusion bodies contain amyloid-like structure. PLoS Biol. 6, e195.

[53] Guijarro, J.I., Sunde, M., Jones, J.A., Campbell, I.D. and Dobson, C.M. (1998) Amyloid fibril formation by an SH3 domain. Proc. Natl. Acad. Sci. USA 95, 4224–4228.

[54] Chiti, F., Webster, P., Taddei, N., Clark, A., Stefani, M., Ramponi, G. and Dobson, C.M. (1999) Designing conditions for in vitro formation of amyloid protofilaments and fibrils. Proc. Natl. Acad. Sci. USA 96, 3590–3594.

[55] Dobson, C.M. (2001) The structural basis of protein folding and its links with human disease. Philos. Trans. R. Soc. Lond. B Biol. Sci. 356, 133–145.

[56] Nelson, R. and Eisenberg, D. (2006) Recent atomic models of amyloid fibril structure. Curr. Opin. Struct. Biol. 16, 260–265.

[57] Tjernberg, L., Hosia, W., Bark, N., Thyberg, J. and Johansson, J. (2002) Charge attraction and beta propensity are necessary for amyloid fibril formation from tetrapeptides. J. Biol. Chem. 277, 43243–43246.

[58] Margittai, M. and Langen, R. (2006) Side chain-dependent stacking modulates tau filament structure. J. Biol. Chem. 281, 37820–37827.

[59] Zanuy, D. and Nussinov, R. (2003) The sequence dependence of fiber organization. A comparative molecular dynamics study of the islet amyloid polypeptide segments 22–27 and 22–29. J. Mol. Biol. 329, 565–584.

[60] Fernandez-Escamilla, A.M., Rousseau, F., Schymkowitz, J. and Serrano, L. (2004) Prediction of sequence-dependent and mutational effects on the aggregation of peptides and proteins. Nat. Biotechnol. 22, 1302–1306.

[61] Tartaglia, G.G., Pawar, A.P., Campioni, S., Dobson, C.M., Chiti, F. and Vendruscolo, M. (2008) Prediction of aggregation-prone regions in structured proteins. J. Mol. Biol. 380, 425–436.

[62] Polverino de Laureto, P., Taddei, N., Frare, E., Capanni, C., Costantini, S., Zurdo, J., Chiti, F., Dobson, C.M. and Fontana, A. (2003) Protein aggregation and amyloid fibril formation by an SH3 domain probed by limited proteolysis. J. Mol. Biol. 334, 129–141.

[63] Marcon, G., Plakoutsi, G., Canale, C., Relini, A., Taddei, N., Dobson, C.M., Ramponi, G. and Chiti, F. (2005) Amyloid formation from HypF-N under conditions in which the protein is initially in its native state. J. Mol. Biol. 347, 323–335.

[64] Eisenberg, D., Nelson, R., Sawaya, M.R., Balbirnie, M., Sambashivan, S., Ivanova, M.I., Madsen, A.O. and Riekel, C. (2006) The structural biology of protein aggregation diseases: fundamental questions and some answers. Acc. Chem. Res. 39, 568–575.

[65] Bennett, M.J., Sawaya, M.R. and Eisenberg, D. (2006) Deposition diseases and 3D domain swapping. Structure 14, 811–824.

[66] Valéry, C., Paternostre, M., Robert, B., Gulik-Krzywicki, T., Narayanan, T., Dedieu, J.C., Keller, G., Torres, M.L., Cherif-Cheikh, R., Calvo, P. and Artzner, F. (2003) Biomimetic organization: octapeptide self-assembly into nanotubes of viral capsid-like dimension. Proc. Natl. Acad. Sci. USA 100, 10258–10262.

[67] Ryadnov, M.G. (2007) Peptide alpha-helices for synthetic nanostructures. Biochem. Soc. Trans. 35, 487–491.

[68] Dvir, H., Lundberg, M.E., Maji, S.K., Riek, R. and Choe, S. (2009) Mistic: cellular localization, solution behavior, polymerization, and fibril formation. Protein Sci. 18, 1564–1570.

[69] Wiltzius, J.J., Sievers, S.A., Sawaya, M.R., Cascio, D., Popov, D., Riekel, C. and Eisenberg, D. (2008) Atomic structure of the cross-beta spine of islet amyloid polypeptide (amylin). Protein Sci. 17, 1467–1474.

[70] Antzutkin, O.N., Leapman, R.D., Balbach, J.J. and Tycko, R. (2002) Supramolecular structural constraints on Alzheimer's beta-amyloid fibrils from electron microscopy and solid-state nuclear magnetic resonance. Biochemistry 41, 15436–15450.

[71] Jaroniec, C.P., MacPhee, C.E., Astrof, N.S., Dobson, C.M. and Griffin, R.G. (2002) Molecular conformation of a peptide fragment of transthyretin in an amyloid fibril. Proc. Natl. Acad. Sci. USA 99, 16748–16753.

[72] Petkova, A.T., Buntkowsky, G., Dyda, F., Leapman, R.D., Yau, W.M. and Tycko, R. (2004) Solid state NMR reveals a pH-dependent antiparallel beta-sheet registry in fibrils formed by a beta-amyloid peptide. J. Mol. Biol. 335, 247–260.

[73] Kammerer, R.A., Kostrewa, D., Zurdo, J., Detken, A., Garcia-Echeverria, C., Green, J.D., Muller, S.A., Meier, B.H., Winkler, F.K., Dobson, C.M. and Steinmetz, M.O. (2004) Exploring amyloid formation by a de novo design. Proc. Natl. Acad. Sci. USA 101, 4435–4440.

[74] Iwata, K., Fujiwara, T., Matsuki, Y., Akutsu, H., Takahashi, S., Naiki, H. and Goto, Y. (2006) 3D structure of amyloid protofilaments of beta2-microglobulin fragment probed by solid-state NMR. Proc. Natl. Acad. Sci. USA 103, 18119–18124.

[75] Tycko, R., Sciarretta, K.L., Orgel, J.P. and Meredith, S.C. (2009) Evidence for novel-sheet structures in Iowa-mutant beta – amyloid fibrils. Biochemistry 48, 6072–6084.

[76] Paravastu, A.K., Qahwash, I., Leapman, R.D., Meredith, S.C. and Tycko, R. (2009) Seeded growth of {beta}-amyloid fibrils from Alzheimer's brain-derived fibrils produces a distinct fibril structure. Proc. Natl. Acad. Sci. USA 106, 7443–7448.

[77] Heise, H., Hoyer, W., Becker, S., Andronesi, O.C., Riedel, D. and Baldus, M. (2005) Molecular-level secondary structure, polymorphism, and dynamics of full-length alpha-synuclein fibrils studied by solid-state NMR. Proc. Natl. Acad. Sci. USA 102, 15871–15876.

[78] Baxa, U., Wickner, R.B., Steven, A.C., Anderson, D.E., Marekov, L.N., Yau, W.M. and Tycko, R. (2007) Characterization of beta-sheet structure in Ure2p1–89 yeast prion fibrils by solid-state nuclear magnetic resonance. Biochemistry 46, 13149–13162.

[79] Chan, J.C., Oyler, N.A., Yau, W.M. and Tycko, R. (2005) Parallel beta-sheets and polar zippers in amyloid fibrils formed by residues 10–39 of the yeast prion protein Ure2p. Biochemistry 44, 10669–10680.

[80] Luca, S., Yau, W., Leapman, R. and Tycko, R. (2007) Peptide conformation and supramolecular organization in amylin fibrils: constraints from solid-state NMR. Biochemistry 46, 13505–13522.

[81] Nielsen, J.T., Bjerring, M., Jeppesen, M.D., Pedersen, R.O., Pedersen, J.M., Hein, K.L., Vosegaard, T., Skrydstrup, T., Otzen, D.E. and Nielsen, N.C. (2009) Unique identification of supramolecular structures in amyloid fibrils by solid-state NMR spectroscopy. Angew. Chem., Int. Ed. Engl. 48, 2118–2121.

[82] Madine, J., Jack, E., Stockley, P.G., Radford, S.E., Serpell, L.C. and Middleton, D.A. (2008) Structural insights into the polymorphism of amyloid-like fibrils formed by region 20–29 of amylin revealed by solid-state NMR and X-ray fiber diffraction. J. Am. Chem. Soc. 130, 14990–15001.

[83] Shewmaker, F., Wickner, R.B. and Tycko, R. (2006) Amyloid of the prion domain of Sup35p has an in-register parallel beta-sheet structure. Proc. Natl. Acad. Sci. USA 103, 19754–19759.

[84] Wickner, R.B., Dyda, F. and Tycko, R. (2008) Amyloid of Rnq1p, the basis of the [PIN+] prion, has a parallel in-register beta-sheet structure. Proc. Natl. Acad. Sci. USA 105, 2403–2408.

[85] Helmus, J.J., Surewicz, K., Nadaud, P.S., Surewicz, W.K. and Jaroniec, C.P. (2008) Molecular conformation and dynamics of the Y145Stop variant of human prion protein in amyloid fibrils. Proc. Natl. Acad. Sci. USA 105, 6284–6289.

[86] Laws, D.D., Bitter, H.M.L., Liu, K., Ball, H.L., Kaneko, K., Wille, H., Cohen, F.E., Prusiner, S.B., Pines, A. and Wemmer, D.E. (2001) Solid-state NMR studies of the secondary structure of a mutant prion protein fragment of 55 residues that induces neurodegeneration. Proc. Natl. Acad. Sci. USA 98, 11686–11690.

[87] Lim, K.H., Nguyen, T.N., Damo, S.M., Mazur, T., Ball, H.L., Prusiner, S.B., Pines, A. and Wemmer, D.E. (2006) Solid-state NMR structural studies of the fibril form of a mutant mouse prion peptide PrP89–143(P101L). Solid State Nucl. Magn. Reson. 29, 183–190.

[88] Kuwata, K., Matumoto, T., Cheng, H., Nagayama, K., James, T.L. and Roder, H. (2003) NMR-detected hydrogen exchange and molecular dynamics simulations provide structural insight into fibril formation of prion protein fragment 106–126. Proc. Natl. Acad. Sci. USA 100, 14790–14795.

[89] Ferguson, N., Becker, J., Tidow, H., Tremmel, S., Sharpe, T.D., Krause, G., Flinders, J., Petrovich, M., Berriman, J., Oschkinat, H. and Fersht, A.R. (2006) General structural motifs of amyloid protofilaments. Proc. Natl. Acad. Sci. USA 103, 16248–16253.

[90] Olofsson, A., Ippel, J.H., Wijmenga, S.S., Lundgren, E. and Ohman, A. (2004) Probing solvent accessibility of transthyretin amyloid by solution NMR spectroscopy. J. Biol. Chem. 279, 5699–5707.

[91] Olofsson, A., Sauer-Eriksson, A.E. and Ohman, A. (2006) The solvent protection of alzheimer amyloid-beta-(1–42) fibrils as determined by solution NMR spectroscopy. J. Biol. Chem. 281, 477–483.

[92] Olofsson, A., Lindhagen-Persson, M., Sauer-Eriksson, A.E. and Ohman, A. (2007) Amide solvent protection analysis demonstrates that amyloid-beta(1–40) and amyloid-beta(1–42) form different fibrillar structures under identical conditions. Biochem. J. 404, 63–70.

[93] Verel, R., Tomka, I.T., Bertozzi, C., Cadalbert, R., Kammerer, R.A., Steinmetz, M.O. and annd Meier, B.H. (2008) Polymorphism in an amyloid-like fibril-forming model peptide. Angew. Chem., Int. Ed. Engl. 47, 5842–5845.

[94] Alexandrescu, A.T. (2001) An NMR-based quenched hydrogen exchange investigation of model amyloid fibrils formed by cold shock protein A. Pac. Symp. Biocomput., 67–78.

[95] Ippel, J.H., Olofsson, A., Schleucher, J., Lundgren, E. and Wijmenga, S.S. (2002) Probing solvent accessibility of amyloid fibrils by solution NMR spectroscopy. Proc. Natl. Acad. Sci. USA 99, 8648–8653.

[96] Madine, J., Copland, A., Serpell, L.C. and Middleton, D.A. (2009) Cross-beta spine architecture of fibrils formed by the amyloidogenic segment NFGSVQFV of medin from solid-state NMR and X-ray fiber diffraction measurements. Biochemistry 48, 3089–3099.

[97] Lee, S.W., Mou, Y., Lin, S.Y., Chou, F.C., Tseng, W.H., Chen, C.H., Lu, C.Y., Yu, S.S. and Chan, J.C. (2008) Steric zipper of the amyloid fibrils formed by residues 109–122 of the Syrian hamster prion protein. J. Mol. Biol. 378, 1142–1154.

[98] Wilson, L.M., Mok, Y.F., Binger, K.J., Griffin, M.D., Mertens, H.D., Lin, F., Wade, J.D., Gooley, P.R. and Howlett, G.J. (2007) A structural core within apolipoprotein C-II amyloid fibrils identified using hydrogen exchange and proteolysis. J. Mol. Biol. 366, 1639–1651.

[99] Bu, Z., Shi, Y., Callaway, D.J. and Tycko, R. (2007) Molecular alignment within beta-sheets in Abeta(14–23) fibrils: solid-state NMR experiments and theoretical predictions. Biophys. J. 92, 594–602.

[100] Whittemore, N.A., Mishra, R., Kheterpal, I., Williams, A.D., Wetzel, R. and Serpersu, E.H. (2005) Hydrogen-deuterium (H/D) exchange mapping of Abeta 1–40 amyloid fibril secondary structure using nuclear magnetic resonance spectroscopy. Biochemistry 44, 4434–4441.

[101] Naito, A., Kamihara, M., Inoue, R. and Saitô, H. (2004) Structural diversity of amyloid fibril formed in human calcitonin as revealed by site-directed 13C solid-state NMR spectroscopy. Magn. Reson. Chem. 42, 247–257.